MOEMS Thermal Imaging Camera

M. Fatih Toy, Onur Ferhanoglu, Hamdi Torun, F. Levent Degertekin*, Hakan Urey*
Department of Electrical Engineering, Koç University, Istanbul-Turkey
*Georgia Institute of Technology, Atlanta-USA

Abstract— **A novel thermo-mechanical Infrared (IR) imaging array with integrated diffraction gratings for optical readout was fabricated and tested. Parylene was used as a structural material for its low thermal conductivity and high thermal expansion properties. Tests were performed using an IR blackbody target and first order diffracted light was imaged on a CCD camera to monitor the entire array. Results show that it is possible to achieve <100mK NETD using a 12 bit CCD camera.**

I. INTRODUCTION

Thermal imaging has been utilized in many temperature monitoring applications such as surveillance, defense, biomedical imaging, monitoring circuits /machinery, and rescue. Cooled and uncooled thermal imaging methods are the two main approaches to thermal imaging. Uncooled thermal imaging has the advantages of low cost and fabrication simplicity with poorer performance compared to cooled approach. Operational principle of uncooled thermal imagers is based on the detection of an output, either electrical or mechanical, that is modulated with the absorbed IR heat. Micro Electro-mechanical System (MEMS) based uncooled thermomechanical detectors are used to monitor optical or electrical outputs caused by mechanical bending or rotation of a bimaterial structure due to absorbed IR radiation. In the group of MEMS based uncooled thermomechanical detectors, optical readout methods are superior to other methods in the sense of sensitivity [1] and elimination of electrical interconnects.

In this work; design, fabrication and performance of an uncooled thermomechanical detector is explained. Noise performance of detector is observed with an integrated diffraction grating underneath each element, monitoring 1st diffraction orders using a CCD camera. Furthermore, the effect of material choice on the performance is explored. Parylene is one of the most suitable structural materials with its high coefficient of thermal expansion (CTE) and thermal resistivity.

II. THEORY

Bimaterial thermal detector performance is composed from a group of parameters such as; IR absorbance, stiffness, thermal isolation, bending or rotation per temperature increase.

A. Noise Analysis

The performance of uncooled bimaterial IR imager arrays is limited by temperature fluctuation noise, background fluctuation noise, thermo-mechanical noise. Datskos et al developed analytical measures for all three components of NETD [1]:

Thermal fluctuations are caused due to the heat exchange between the pixel and its environment, and the NETD due to thermal fluctuations can be expressed as [2]:

$$\mathrm{NETD}_{\mathrm{TF}} = \frac{8 f^2 T_D \sqrt{k_B G B}}{\eta \tau_0 A_d \left(dP/dT\right)_{\lambda_1-\lambda_2}} \qquad (1)$$

where f is the f-number of the IR optics, T_D is detector temperature, k_B is Boltzmann's constant, G is the thermal conductance, B is measurement bandwidth, η is the absorbance of the detector, τ_0 is the transmission of optics, A_d is the surface are of the detector (area of the absorbing region) and dP/dT is the change of power with respect to temperature within the given wavelength range.

The fundamental limit of the thermal fluctuation noise arises due to the radiative heat exchange between the pixel and surroundings, so called the background fluctuation noise. NETD due to background calculations is expressed as [2]:

$$\mathrm{NETD}_{\mathrm{BF}} = \frac{8 f^2}{\eta \tau_0 \left(dP/dT\right)_{\lambda_1-\lambda_2}} \sqrt{\frac{2 k_B \sigma_T B (T_D^5 + T_B^5)}{A_d}} \qquad (2)$$

where σ_T is Stephan-Boltzmann constant and, T_B is the background temperature.

Thermo-mechanical noise is caused due to the continuous exchange of the mechanical energy accumulated in the device and the thermal energy of the environment and the NETD due to thermo-mechanical fluctuations can be expressed as [2]:

This work is partly sponsored by Aselsan.

$$\mathrm{NETD}_{\mathrm{TM}} = \frac{8 f^2 G}{\eta \tau_0 A_d \left(dP/dT\right) \lambda_1 - \lambda_2 \left(dz/dT\right)} \sqrt{\frac{k_B T_D B}{kQ\omega_0}} \quad (3)$$

where dz/dT is the mechanical responsivity of the detector to unit temperature increase on the detector, k, Q, w_0 are spring constant, quality factor and resonant frequency of the structure respectively.

Moreover, NETD due to optical readout [3] is expressed as:

$$NETD_{RO} = \frac{dz/dT}{T_d/T_t} \frac{n_{CCD}}{S_{CCD}} \quad (4)$$

where T_d / T_t is the value of temperature change on the detector caused by unit temperature change at the target, n_{CCD} is the noise of the CCD camera, and S_{CCD} is the sensitivity of the detector as the ratio of readout intensity variation in the CCD units per unit deflection of the detector. CCD sensitivity and noise values vary with the selection of camera, so CCD device is considered to have 12 bits of dynamic range for theoretical NETD calculations. Overall NETD is calculated using:

$$\mathrm{NETD} = \sqrt{\mathrm{NETD}_{\mathrm{TF}}^2 + \mathrm{NETD}_{\mathrm{BF}}^2 + \mathrm{NETD}_{\mathrm{TM}}^2 + \mathrm{NETD}_{\mathrm{RO}}^2} \quad (7)$$

Fig. 1 shows different detector designs, and calculated NETD for each design is given in Table 1.

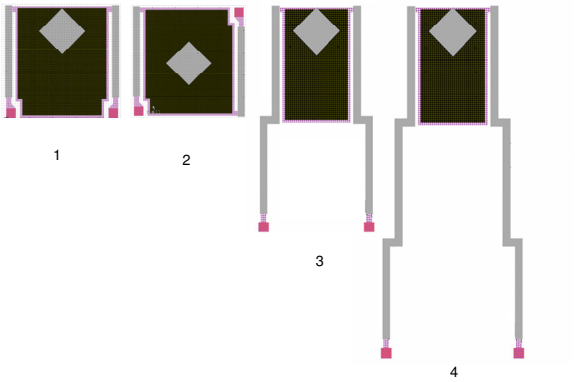

Figure 1. Various detector designs with different performances, performance comparison is given in Table 1

TABLE I. THEORETICAL NETD VALUES FOR DIFFERENT DETECTOR DESIGNS

Design	$\mathrm{NETD}_{\mathrm{TF}}$ (mK)	$\mathrm{NETD}_{\mathrm{BF}}$ (mK)	$\mathrm{NETD}_{\mathrm{TM}}$ (mK)	$\mathrm{NETD}_{\mathrm{RO}}$ (mK)	$\mathrm{NETD}_{\mathrm{TOTAL}}$ (mK)
1	2.7	2.9	6.7	16.1	17.9
2	18.7	2.9	8.3	175	176
3	2.6	3.2	8.3	4.5	10.3
4	1.9	3.2	8.3	1.9	9.2

III. FABRICATION

A. *Fabrication Steps*

The devices were fabricated at the Microelectronics Research Center at Georgia Institute of Technology. Quartz wafers were used to serve as a transparent medium for the optical readout.

The gratings were evaporated and patterned on the substrate. Photoresist (PR) was used as a sacrificial layer to serve as a quarter wavelength gap in between the bottom metal and IR absorber to enhance absorption. Parylene dimmer was evaporated on top of the sacrificial layer as a structural material. Titanium was sputtered and patterned to serve as the secondary bimaterial pair. A thin layer of titanium was sputtered on top of the devices for IR absorption. Final step of the fabrication is given in Fig. 2. Microscope photograph of the fabricated array is shown in Fig. 3.

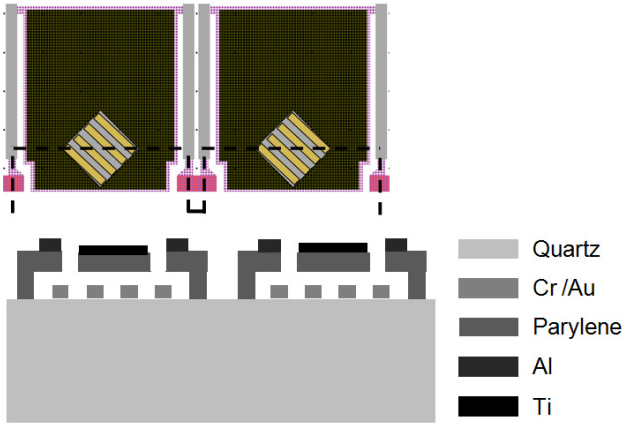

Figure 2.Final step of detector fabrication

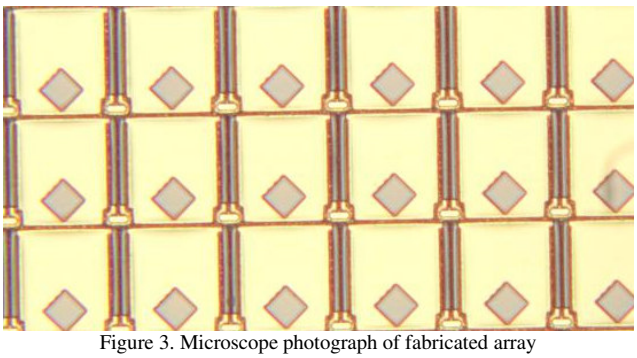

Figure 3. Microscope photograph of fabricated array

IV. EXPERIMENTAL SETUP

Fabricated detector array is enclosed into a vacuum package which has an infrared window and a visible readout window. A He-Ne laser as the readout source is expanded to match with the size of the detector array and directed to the detector substrate through the visible window. Diffracted

light returning from the detector array is band pass filtered to only transmit 1st diffraction order from every detector element and imaged on to an 8 bit CCD camera operating with a shutter speed of 33ms and a frame rate of 15 fps. A shutter is placed in front of a heater with high emissivity tape staring at the detectors through the infrared window. Fig. 4 shows the optical readout setup.

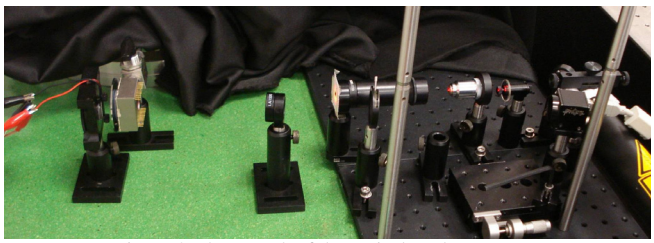

Figure 4. Photograph of the optical readout setup

V. Results and Discussion

CCD camera at the readout setup is used to monitor the 1st diffraction order intensity modulation from detector elements. Diffracted light from each detector element is imaged on to a group of CCD pixels. Fig. 5 shows a snapshot from the CCD camera output.

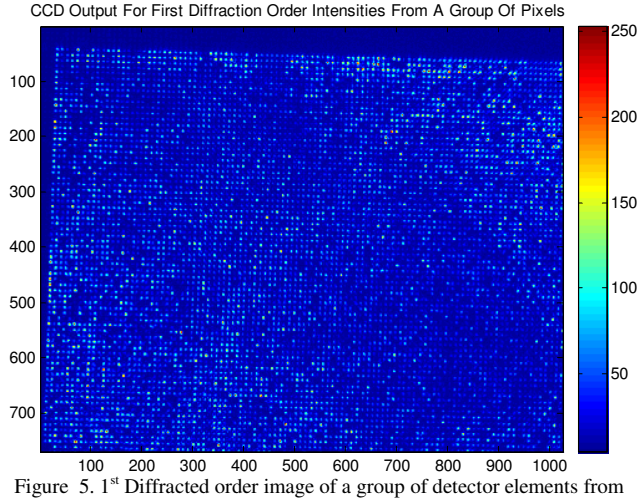

Figure 5. 1st Diffracted order image of a group of detector elements from the CCD camera.

With the off chip pixel binning for the CCD pixels receiving light from the same detector element, dynamic range of the CCD camera is enhanced to 10 bits. In order to measure experimental NETD, temperature of the heater is increased to 155°C. Then the heater is blocked by a shutter at the room temperature (25°C). Binned output from the CCD camera for a selected detector element is recorded during the experiment. Fig. 6 shows a sample CCD output for a selected pixel for this target temperature change.

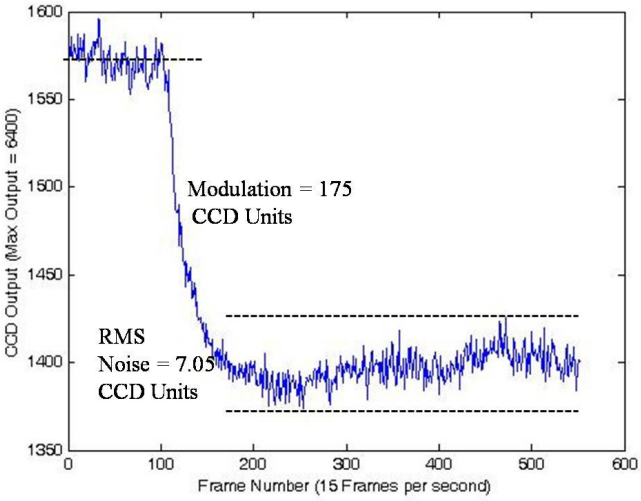

Figure 6. CCD Output modulation by the change of target temperature for a selected detector element.

From the data in Fig. 6, SNR can be found as 24.8. The increase in the IR target temperature is 130°K, therefore the NETD of this pixel is calculated as 5.24°K using ~*f*/1.5 optics for the light collection system. The reason for this mismatch between theoretical and experimental results was further explored, and it was realized that the self modulation of the readout source and the leak of the vacuum package are the dominating noise sources. These noise sources were not studied in the previous chapters, because the self modulation of the readout source, which appears as a cyclic modulation on the Fig. 6 can be completely eliminated with the application of a simple correlated double sampling method. Furthermore, the leak from the vacuum package causes the drift of output at Fig. 6. Permanent sealing of the vacuum package can stop the leak and this drift behavior. With the corrections for these two factors, experimental NETD is recalculated as 2.3°K.

VI. Conclusion and Future Work

Parylene based thermal imaging array was designed, fabricated and tested. Experiments reveal that 2.3 °K is achieved for the proposed design, which is close to theoretical findings for the same test conditions. Incorporation of a 12bit CCD camera into experimental setup using f/1 optics should allow achieving an NETD of <100°mK, and further improvements in the experimental setup are planned as the future work.

Acknowledgment

This work is partly sponsored by ASELSAN (Turkey). We'd like to acknowledge the support from NSF International collaboration grant (award number: 0423403) and the MiRC staff at Georgia Tech.

REFERENCES

[1] W. Lee, N.A. Hall and F.L. Degertekin, "A grating-assisted resonant-cavity-enhanced optical displacement detection method for micromachined sensors", Appl .Phys. Lett. 3032 , 2004

[2] P.G. Datskos, N.V.Lavrik, S.Rajic, "Performance of uncooled microcantilever thermal detectors", Review of Scientific Instruments, vol. 75, no. 4, 2004.

[3] Y. Zhao, "Optomechanical Uncooled Infrared Imaging System", Dissertation for the Degree of Doctor of Philosophy, University of California, Berkeley, Fall 2002.